T.V. KONONENKO[1],✉
M. MEIER[2]
M.S. KOMLENOK[1]
S.M. PIMENOV[1]
V. ROMANO[2]
V.P. PASHININ[1]
V.I. KONOV[1]

Microstructuring of diamond bulk by IR femtosecond laser pulses

[1] General Physics Institute, Vavilov str. 38, 119991 Moscow, Russia
[2] Institute of Applied Physics, University of Bern, Sidlerstrasse 5, 3012 Bern, Switzerland

ABSTRACT We report the fabrication of graphitic microstructures in the bulk of chemical vapor deposited (CVD) diamond using 120-fs laser pulses at 800-nm wavelength. The nature of the laser-modified region and generation of mechanical stresses in the surrounding diamond is studied with Raman spectroscopy. A spontaneous growth of the laser-modified region from the focal plane towards the laser has been visualized in the process of multipulse irradiation with different pulse energies. The formation of discrete or continuous graphitized structures is revealed depending on the varied local laser intensity. The physical processes governing the appearance of separate graphitic globules and continuous extension of the graphitized region are discussed. Controlling the laser irradiation conditions permits us to fabricate graphitic wires with typical length of 150 µm and diameter of 1.5 µm. The longer, 300-ps pulses, as applied to laser microstructuring of the CVD diamond bulk, are found to be inappropriate due to the stronger influence of structural defects on the damage threshold, the noticeable fluctuation of the structure diameter over the length and the pronounced cracking of the surrounding diamond.

PACS 42.62.-b; 61.80.Ba

1 Introduction

The extensive capabilities of femtosecond laser pulses for the generation of various microstructures in the bulk of different transparent materials like glasses and photoresistors were demonstrated recently [1–8]. The possible laser-induced phenomena include generation of color centers, change of refractive index due to densification and defect formation, appearance of microvoids due to remelting and shock waves, cracking due to destructive breakdown, etc. These material-specific effects were utilized for fabrication of three-dimensional optical memories with ultra-high storage density [1], optical circuits [2–4], photonic nanostructures [5], surface relief gratings [6] and volume Fresnel zone plates [7].

Laser-induced phase transition in diamond opens unique opportunities for bulk microstructuring of the material. The

✉ Fax: +7-499-503-81-51, E-mail: kononen@nsc.gpi.ru

drastic differences in optical and electrical properties of the original material (diamond) compared to the modified material (graphite) make it appear very promising for the design of various optical, photonic and electronic devices. A few examples of inner diamond graphitization induced by pulsed laser irradiation were already reported including the formation of buried graphitic layers in ion-implanted diamond [9, 10] and graphitic channels with typical diameter of 20 µm [11]. However, many basic physical questions concerning the occurrence and growth of graphitized microstructures in the bulk of diamond still require deeper investigation. One of the problems arises from the noticeable difference in the densities between diamond (3.5 g/cm^3) and graphite (1.8–2.25 g/cm^3), which leads to an expansion of the material at the diamond–graphite phase transition. A simple theoretical estimation in [12] predicts that the appearance of even a nanometer-scale graphitic globule inside the diamond matrix initiates enough tensile stress to cause diamond cracking. Such an effect could substantially limit the perspectives of diamond bulk microstructuring; so, it requires careful experimental verification. Among other important questions, the effect of laser pulse duration on the phase-transition process in the bulk of diamond is to be clarified, as has been done earlier for the surface graphitization of diamond [13]. Artificial diamond produced by chemical vapor deposition (CVD) is much cheaper and more accessible than the natural diamond, so it is more attractive for possible industrial applications. However, the polycrystalline nature of the CVD diamond makes it necessary to specify the influence of the local structure fluctuations on controllability of the laser processing.

This paper reports the formation of graphitized globules and high-aspect-ratio wires with the specific diameter of a few micrometers in the bulk of CVD diamond utilizing IR femtosecond laser pulses. We have studied the influence of the material and the irradiation conditions on the optical breakdown, which initiates the laser-induced diamond microstructuring. The structure of the laser-modified region and surrounding diamond is investigated with Raman spectroscopy. A spontaneous growth of the modified region under multipulse irradiation is visualized for different radiation parameters; physical processes defining the growth dynamics are considered. The microstructures produced by 120-fs pulses and 300-ps pulses at similar irradiation conditions are compared.

2   Experiments

A sample of $1 \times 1 \times 5$ mm^3 size with polished sides was prepared from optical quality CVD diamond grown in microwave plasma [14]. The laser pulses with duration of 120 fs were generated by a regenerative amplified mode-locked Ti:sapphire laser (Spectra Physics) operating at a wavelength of 800 nm. The experiments on laser structuring of diamond bulk were performed with a 8-mm objective, which provided the beam waist diameter of 3.0 μm measured at an intensity level of $1/e$. In the experiments with the 300-ps pulses (1064-nm wavelength) generated by a mode-locked Nd:YAG laser the beam waist diameter was 3.6 μm. A ×50 microscopic objective and a CCD camera were used to visualize and record the appearance of light-absorbing (dark) structures near the focal point, which was shifted typically at 50–250 μm distance from the surface into the bulk of the diamond sample. The laser-affected region was observed perpendicularly to the laser beam.

Two 0.5-mm-thick polished plates of the optical quality CVD diamond and natural IIa type single crystal diamond were prepared for optical transmittance measurements. The laser light transmittance was measured as a function of the laser fluence ranging from the laser damage threshold down to the value two orders of magnitude lower than the laser damage threshold. A central, nearly uniform part of the laser beam was cut off by a round diaphragm and imaged by a 200-mm lens at the sample surface in a spot of 65 μm. As a result, the laser fluence was kept at an almost constant level both over the whole irradiation spot area and through the sample thickness.

Raman microanalysis was carried out with a self-made setup consisting of a double monochromator (Jobin-Yvon HRD1) and a single photon avalanche diode (PerkinElmer SPCM-AQ). Raman scattering was excited by continuous radiation of a diode-pumped frequency-doubled Nd:YVO laser at the wavelength of 532 nm. A narrow-band dielectric filter reduced the laser line width to 0.3 nm (FWHM). A ×40 microscopic objective was used to focus the exciting radiation inside the diamond sample and to collect the scattered light.

3   Results

3.1   *Optical breakdown in diamond*

It is generally recognized that the advantages of femtosecond laser pulses in processing of transparent mate-

rials are based on the increased efficiency of nonlinear photoionization providing direct excitation of electrons from the valence band to the conduction band by the laser field. Depending on the laser frequency and intensity, multiphoton ionization or tunneling ionization becomes dominant. Another important parameter is the band gap of a transparent material [15, 16]. If the band gap is relatively small, the nonlinear photoionization alone is sufficient to reach the critical electron density, which provides efficient absorption of the laser radiation and leads to irreversible changes in the material structure. On the contrary, for large-band-gap materials, the avalanche impact ionization produces most of the free electrons required for the optical breakdown. However, nonlinear photoionization still enlarges the concentration of seed electrons and reduces the influence of imperfections of local material structure (defects, impurities, etc.).

Diamond is an indirect-band-gap material with the minimal energy gap of $E_g^{in} = 5.49$ eV and the direct energy gap of $E_g^{dir} = 7.3$ eV [17]. Nonlinear photoionization of diamond by UV femtosecond pulses was studied in [18] and two-photon absorption was found to be the dominant effect for the 248-nm wavelength. As for the laser wavelength of 800 nm and the pulse duration of 100 fs utilized in our experiments, one can assume that contributions of nonlinear ionization and impact ionization processes are comparable under the given laser parameters. This follows from comparison of diamond with other transparent materials examined at the same conditions [15, 16]. Diamond mediates between a set of glasses with the band gap of below 4.4 eV, which are ascribed to the small-band-gap materials with dominating nonlinear ionization, and large-band-gap dielectrics like fused silica ($E_g = 9$ eV) and CaF$_2$ ($E_g = 10.2$ eV).

To verify the influence of the structural defects existing in the CVD diamond on the absorption of femtosecond pulses, transmission of the CVD diamond and the natural diamond specimens was measured in a wide range of laser fluences below the breakdown threshold (Fig. 1). No change in the averaged transmission was found for the natural diamond (Fig. 1a) until the diamond–graphite phase transition caused an irreversible transmission fall at 0.4 J/cm^2. As for the CVD diamond, it demonstrated smaller transmission even at the lowest laser fluence (Fig. 1b), presumably due to the presence of absorbing (graphitic) impurities. Besides, a slight reversible reduction of transmission under rise of fluence was observed
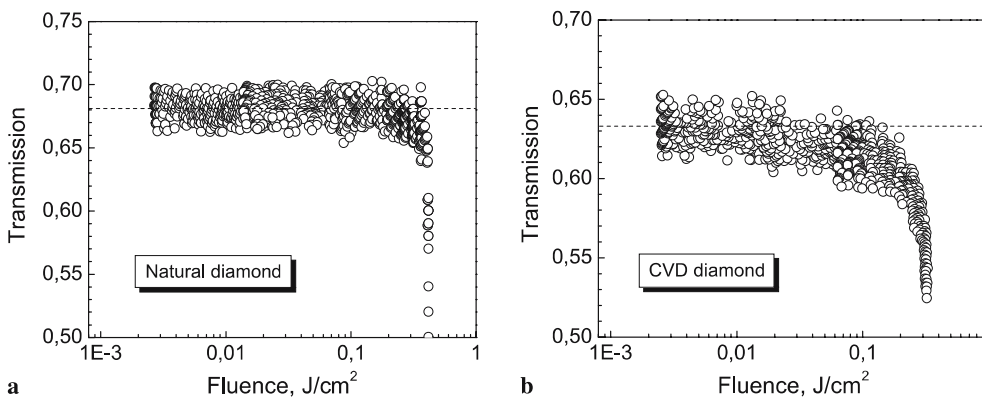

FIGURE 1 Optical transmission of diamond specimens as a function of incident laser fluence for 120-fs pulses: (**a**) natural single crystal diamond, (**b**) CVD diamond

for the CVD diamond before the final fall at 0.3 J/cm²; it can be attributed to increasing photoionization from defect states.

The transmission measurements prove that the defects and impurities in the CVD diamond make a detectable contribution to the ionization process and intensify production of the seed electrons for the impact ionization. This leads to a $\sim 30\%$ reduction of the damage threshold for the CVD diamond compared with the natural diamond. Essentially larger scattering in the thresholds was obtained when the same specimens were irradiated by 300-ps pulses. The damage thresholds for the natural and CVD diamond were 10–80 J/cm² and 2–4 J/cm², respectively, strongly fluctuating under displacement over the specimen surface. Thus, femtosecond pulses provide much better controllability of the CVD diamond processing; however, they do not allow the complete avoidance of the influence of the structural defects.

The feature of the reported transmission measurements was that the applied optical scheme ensured an approximately constant laser fluence through the sample thickness. Under these conditions, the laser damage first occurred at the rear surface of the sample. Moreover, the measured damage threshold was essentially lower than the value obtained under tight beam focusing and small Rayleigh range, which were typical for the experiments on the bulk microstructuring reported below. The phenomenon, already reported for diamond [19], can be explained by interference of incident and reflected light near the rear side of a transparent dielectric medium, which enlarges the laser intensity in a narrow layer and reduces the measured damage threshold [20]. The expected ratio between the damage thresholds for the front and rear sides is determined only by the refractive index [20]: $4n^2/(n+1)^2 \approx 2$ for $n = 2.4$ in the case of diamond. As a consequence, when the optical breakdown occurs near the rear surface of the specimen, the laser intensity in other regions of the irradiated volume is still two times lower than the breakdown threshold. Thus, correct measurement of the laser-induced optical absorption near the breakdown threshold appears impossible for the applied optical scheme.

The appearance of visible damage under tight focusing of the laser beam at the diamond surface or beneath it demonstrates a pronounced 'incubation' effect, i.e. the damage occurs only after several laser shots if the laser fluence is below a certain value – $F_{inc} \approx 4$ J/cm². The minimum number of laser shots required for the damage to occur quickly increases as the laser fluence decreases, as is shown in Fig. 2 describing the 'incubation' effect at the surface focusing. Similar phenomena were observed earlier for various transparent materials [21] including diamond [22]. The reason of the 'incubation' effect is generally recognized as the appearance and accumulation of stable nanoscale defects, which produce an increasing number of seed electrons for the avalanche process [21]. In the case of diamond, the nature of such defects is still not clear. It will be shown below that the 'incubation' effect plays an important role in spontaneous extension of the laser-modified region under multipulse action.

It seems important also to verify a possible effect of the laser beam self-focusing, which occurs when the applied laser power exceeds the critical value given by the expression [23, 24]
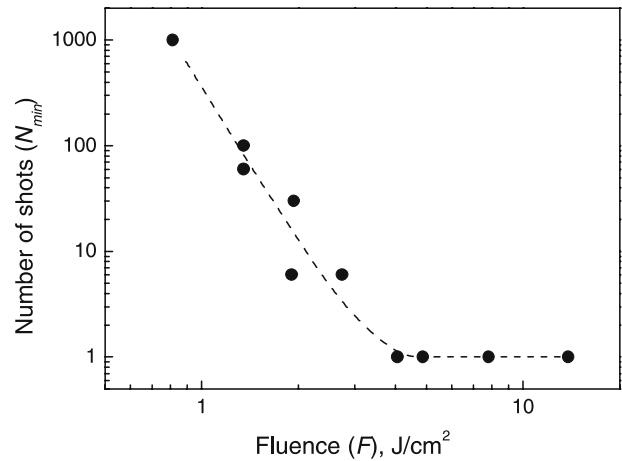

FIGURE 2 Number of laser shots required for the occurrence of visible damage of the diamond surface as a function of laser fluence ('incubation' effect)

$$P_{cr} = 3.77\lambda^2 / (8\pi n_0 n_2) \ , \tag{1}$$

where $\lambda = 800$ nm is the laser wavelength, $n_0 = 2.4$ is the diamond refractive index and $n_2 [\mathrm{cm^2/W}] = (0.0395/4\pi n_0^2) n_2$ [esu] is the nonlinear refraction coefficient of diamond. We applied a linear interpolation to the published data on n_2 [esu] for $\lambda = 1064$ nm $(2.3 \times 10^{-13}$ esu) and $\lambda = 532$ nm, $(4 \times 10^{-13}$ esu) [19] to estimate the nonlinear refraction coefficients at $\lambda = 800$ nm : $n_2 \approx 3.1 \times 10^{-13}$ esu $= 1.69 \times 10^{-16}$ cm²/W. The expression (1) yields the critical laser power value of $P_{cr} = 2.36$ MW. The corresponding level of the laser pulse energy in our experiments is evaluated as $Q_{cr} = P_{cr}\tau/(1-R) = 340$ nJ, where $R = (n_0-1)^2/(n_0+1)^2 = 0.17$ is the reflection from the front surface of the diamond specimen and $\tau = 120$ fs is the pulse duration. All microstructures reported in this article are fabricated at smaller pulse energies, and so we neglect the self-focusing effect under further consideration. This conclusion agrees with the fact that no regular displacement of the initial breakdown position was revealed depending on the laser power applied. Only small $(< 5 \ \mu\mathrm{m})$ stochastic fluctuations of the initial breakdown position were observed, presumably due to material inhomogeneity.

3.2 *Raman spectroscopy of modified region*

Several laser-modified regions produced inside the CVD diamond by a tightly focused beam, as is reported in Sect. 3.3, were investigated with Raman spectroscopy (Fig. 3). The spectrum (bottom) of the original CVD diamond demonstrates a narrow line (1330 cm⁻¹), which is slightly shifted from the position of the first-order Raman spectrum of the undisturbed diamond lattice (1332 cm⁻¹), and a wide peak, which is interpreted as photoluminescence with a maximum at 575.5 nm (2.156 eV) being specific for the nitrogen-containing diamond [25]. The same diamond-related peaks, slightly shifted downward, are observed in the spectrum relating to the laser-modified region, as both exciting and scattered radiation propagate through the surrounding diamond matrix. The top spectrum demonstrates also several
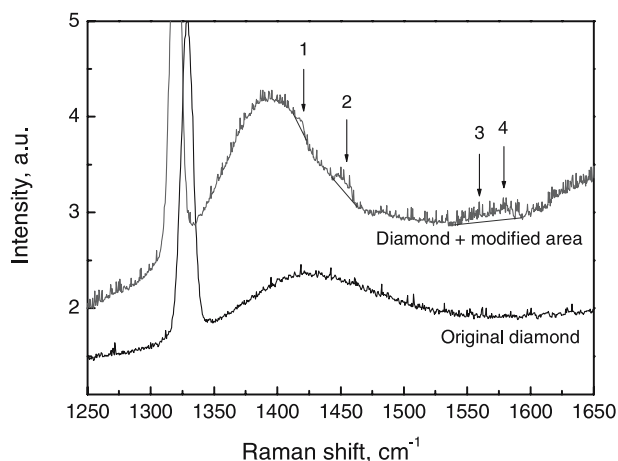
FIGURE 3 Raman spectra of original CVD diamond (*bottom*) and laser-modified region with surrounding diamond (*top*). The four numbered peaks are centered at $1417\,\mathrm{cm}^{-1}$ (1), $1450\,\mathrm{cm}^{-1}$ (2), $1560\,\mathrm{cm}^{-1}$ (3) and $1580\,\mathrm{cm}^{-1}$ (4), respectively

additional low-intensity peaks numbered 1–4 in Fig. 3. The separate peaks centered at $1417\,\mathrm{cm}^{-1}$ (No. 1) and $1450\,\mathrm{cm}^{-1}$ (No. 2) are ascribed to microcrystalline graphite and amorphous sp^2-bounded carbon, respectively [25]. The wide peak in the range of $1540\text{--}1595\,\mathrm{cm}^{-1}$ can be interpreted as two overlapped lines (No. 3 and No. 4) centered at $1560\,\mathrm{cm}^{-1}$ and $1580\,\mathrm{cm}^{-1}$, which belong to microcrystalline graphite [25]. Thus, Raman microanalysis has confirmed our expectations of the diamond–graphite phase transition.

The main diamond peak in the spectrum relating to the modified region is shifted downward by $\Delta \upsilon \approx 10\,\mathrm{cm}^{-1}$ as compared with the original diamond. This shift indicates the appearance of tensile stress in the diamond matrix around the modified region. Indeed, local expansion of the material under the diamond–graphite transition should result in the occurrence of radial compressive stress and tangential biaxial tensile stress in the surrounding diamond. The radial compression seems to be essentially relaxed due to diamond expansion, so it does not affect detectably the Raman spectrum. The value of the biaxial tensile stress (σ) can be evaluated from the measured shift of the peak using the following expression [26, 27]:

$$\Delta \upsilon\,[\mathrm{cm}^{-1}] = -2.05\sigma\,[\mathrm{GPa}]. \qquad (2)$$

The obtained value $\sigma \approx 5\,\mathrm{GPa}$ is much smaller than the theoretical maximum tensile strength for perfect single crystal

diamond (190 GPa), but exceeds most experimental values of the tensile strengths (between 180 and 5190 MPa) measured for various CVD diamond films [28]. The reduction of the tensile strength observed under increase of the film thickness and the grain size was ascribed to microscopic cracks concentrated at the grain boundaries. Let us take into account that the tensile stress generated under standard strength measurements is almost uniform over the specimen thickness, so the film rupture occurs when the stress exceeds a certain threshold. In our experiments, however, the tensile stress is localized near the microscopic modified region. The estimated value of the stress is not sufficient to produce the material fracture inside a diamond grain. The local rise of existing cracks is still possible, but it can be difficult to detect visually. This makes explainable an absence of visible cracks in the diamond matrix around the modified regions produced by femtosecond pulses (see Figs. 4 and 6).

3.3 Spontaneous growth of graphitic structure

When focusing the laser beam beneath the specimen surface, the laser damage first occurs near the focal plane. Multipulse irradiation causes a gradual growth of the modified region towards the laser beam, as illustrated in Fig. 4. In general, the final structure consists of two parts, which under the optical microscope look like (i) a set of irregular dark spots (called further on a 'discrete structure') and (ii) a continuous channel (a 'continuous structure'), which appears later and further from the focal plane.

The dynamics of spontaneous growth of the laser-modified structures under multipulse irradiation was examined using the real-time video of the process. A displacement of the front edge of the modified region from the focus position was presented as a function of the laser shot number. The first derivative of the function was defined as the growth rate. Figure 5 shows variation of the growth rate depending on the distance from the focus position for the structure shown in Fig. 4. The growth-rate curve consists of two parts relating to consecutive formation of the discrete and continuous structures. The change of the growth regime at the distance of $40\,\mu\mathrm{m}$ causes a specific bending of the growth-rate curve, namely, the growth rate quickly decreases before this point, but shows temporal stabilization after it. Summarizing the data on the structures fabricated at various pulse energies, it is found that the transition to the continuous growth regime is observed at a fixed threshold fluence: $F_{\mathrm{th}}^1 = 1.2 \pm 0.2\,\mathrm{J/cm}^2$. Note that this and other evaluations of the local laser fluence
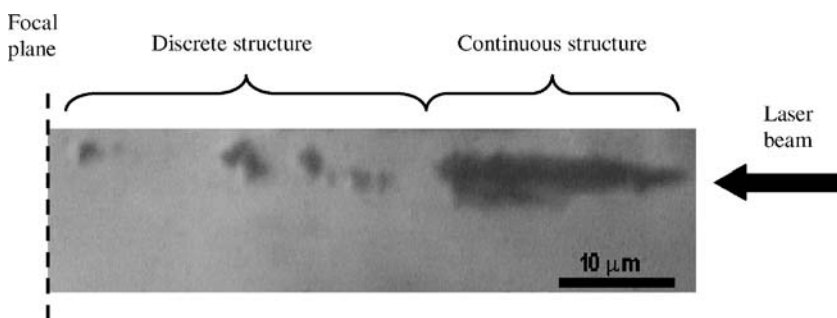

FIGURE 4 Optical microscopy image of laser-modified region inside diamond bulk created by multiple 120-fs pulses with energy of 320 nJ. The position of the focal plane and the direction of laser beam propagation are also shown
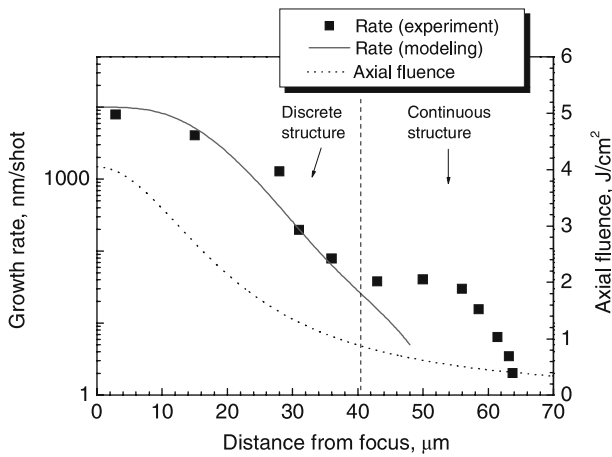
FIGURE 5   Variation of the growth rate under formation of the laser-modified structure shown in Fig. 4 as a function of distance from the focus position. The corresponding change of local laser fluence according to expression (3) and results of 'incubation' effect modeling are also shown

$F(z)$ are obtained via the known expression for an undisturbed Gaussian beam:

$$F(z) = F(0)\omega^2(0)/\omega^2(z) , \tag{3}$$

where z is the distance from the focal plane and $\omega(z)$ is the radius at $1/e$ maximum: $\omega^2(z) = \omega^2(0) + [z\lambda/2\pi\omega(0)]^2$.

The presented observations can be explained by competition of two laser-induced processes. First, it is a breakdown in the original diamond generating a set of separate graphitic globules and, second, it is a continuous extension of the graphitized region initiated by the first process. The observed bending in the growth-rate curve under the change of the dominating process indicates that these two processes are characterized by different dependences of the growth rate on the local laser fluence. At high local fluence $(F > F_{th}^1)$, the appearance of separate graphitic globules at increasing distance from the focus position provides an essentially faster extension of the modified region than the continuous growth. The diamond–graphite phase transition causes a dramatic rise of the optical absorption up to 2×10^5 cm^{-1} [10]; hence, the penetration of the laser radiation behind the graphitized region is completely blocked. This leads to conservation of all graphitic globules excluding the last one fabricated. However, the rate of the discrete structure growth quickly goes down for decreasing fluence until it becomes comparable with the continuous growth rate. The observed weak dependence of the continuous growth rate on the local fluence near F_{th}^1 leads to domination of the continuous growth process at $F < F_{th}^1$. If the laser pulse energy is sufficiently small and the condition $F < F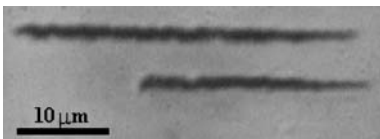_{th}^1$ holds good even in the focal plane, exclusive formation of graphitic wires can be realized, as shown in Fig. 6. The spontaneous growth of a graphitic wire under multipulse irradiation goes on until the local fluence reaches another threshold: $F_{th}^2 = 0.35 \pm 0.05$ J/cm^2. The maximum length of continuous graphitic wires fabricated at fixed irradiation conditions reached 45 μm; this value was limited by a narrow range of appropriate local fluence: $F_{th}^2 < F(z) < F_{th}^1$. However, this limitation could be negotiated via a slow movement of the focus position towards the laser. This approach was used to fabricate 150-μm-long graphitic wires with average diameter of 1.5 μm and typical growth rate of 50–80 nm/shot.

Returning to the occurrence of separate graphitic globules in the diamond, we found that the gradual displacement of the breakdown position from the focus could be well described in the frame of the 'incubation' effect. Indeed, repeated irradiation leads to a reduction of the breakdown threshold, so that the breakdown at increasing distance from the focus becomes possible. This idea is confirmed by good quantitative coincidence of the experimental data on the growth rate for the discrete structure with predictions of a model considering the 'incubation' effect in the diamond bulk (Fig. 5). The model combines the measurements of the 'incubation' period in experiments of the surface irradiation, i.e. the experimental dependence $N_{min}(F)$ in Fig. 2, with the expression (3) for variation of the axial fluence $F(z)$. The resulting dependence $N_{min}(F(z)) = N_{min}(z)$ is converted into the function $z(N_{min})$, which defines an expected position of the laser breakdown depending on the total number of applied laser pulses. Differentiating the last function, we obtain finally the expected rate of the discrete structure growth: $V_{disc}(N) = dz(N_{min})/dN$. For adequate comparison with the experimental data, the expected growth rate is presented in Fig. 5 as a function of the distance from the focus position.

The presented modeling of the 'incubation' effect in the bulk of diamond emphasizes the change in the growth dynamics under the transition from the discrete graphitic globules to the continuous structure. A weak dependence of the growth rate on decreasing local fluence was found to be typical of all examined continuous structures at the initial stage of their formation. In particular, this feature is clearly seen in Fig. 7, which illustrates the growth of a few continuous graphitic
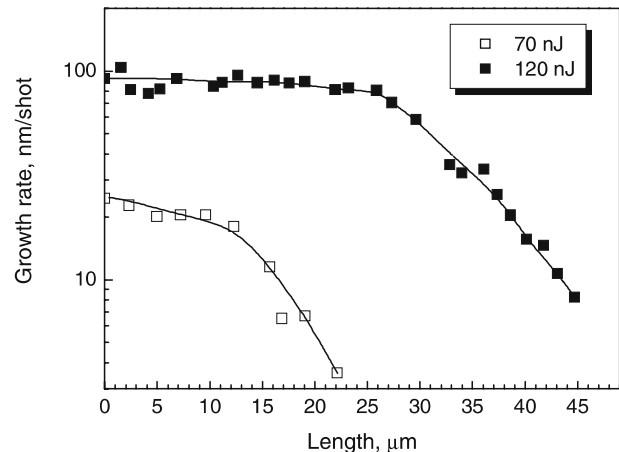

FIGURE 6   Examples of graphitic wires spontaneously grown at fixed irradiation conditions

FIGURE 7   Dynamics of spontaneous growth of continuous graphitic wires at various pulse energies

wires at sufficiently small pulse energies excluding the appearance of the discrete structures. According to the concept presented above, the key process, which determines the dynamics of the discrete structure formation, is the generation of seed electrons for the following avalanche ionization due to nonlinear absorption in diamond and accumulation of easily excited defects under multipulse irradiation. We believe that laser-induced modification of diamond near the front of the existing graphitized region is also based on the avalanche ionization of diamond. However, most seed electrons in this case are generated in graphite instead of diamond, which essentially affects the dynamics of the modified area growth.

The laser light reaching the graphitized area is absorbed in a thin, near-50-nm layer. Graphite has a zero-width band gap and the Fermi level relates to the bottom of the conduction band. The velocity of the electrons excited by photons with energy $h\nu = 1.55$ eV can reach the value of $V_e = \sqrt{2h\nu/m_e} = 7.4 \times 10^7$ cm/s, where $m_e = 9.1 \times 10^{-28}$ g is the electron mass. Hence, hot electrons moving in the ballistic regime, i.e. without any large-angle scattering, can leave graphite and penetrate inside diamond at the maximum distance of $L_e^b \approx 90$ nm during the 120-fs pulse. The measurements of transient thermoreflectivity [29] at thin gold films have demonstrated that fast ballistic movement of photoexcited electrons actually plays an essential role at such small distances. The limited propagation distance of external electrons in diamond restricts the thickness of the layer where the laser-induced avalanche ionization and the formation of light-absorbing plasma can occur. It is necessary to take into account that the concentration of the external electrons inside the enriched diamond layer decreases with distance from the graphite–diamond interface. Hence, the thickness of the diamond layer, where the concentration of the external electrons exceeds the threshold value sufficient to initiate the laser breakdown, must depend on the absorbed (local) energy density in the general case. One can expect a noticeable rise of the modified layer thickness when the local laser fluence increases from F_{th}^1. However, this rise must decelerate and finally stop when the modified layer thickness approaches the maximum, i.e. L_e^b. Thus, the given qualitative model explains the experimental behavior of the continuous growth rate depending on the laser fluence.

More accurate consideration should take into account also post-pulse dissipation of the absorbed energy from the initial ionization zone. Spreading of the energy due to diffusion of hot electrons or thermal conductivity can cause, in principle, an additional growth of the graphitized region. The lifetime of photoexcited electrons in CVD diamond reaches several hundreds of picoseconds [30]; however, most of the absorbed energy is transferred from the electrons to the lattice in the time domain of $\tau_{ei} = 5$–10 ps according to numerous theoretical and experimental studies (see for instance [31, 32]). The diffusion coefficient for electrons excited by picosecond laser pulses in CVD diamond has been experimentally evaluated [30] as $D_e = 6$–9 cm^2/s. Hence, the specific length of post-pulse diffusion of the hot electrons can be roughly estimated as $L_e^d \approx \sqrt{D_e \tau_{ei}} = 50$–$90$ nm. The heat wave generated during the same period (τ_{ei}) propagates at a smaller distance: $L_h \approx \sqrt{\chi \tau_{ei}} \approx 20$–$30$ nm, where $\chi = K/(C_p \varrho) = 0.8$ cm^2/s, $K = 530$ W/(m K) is the thermal conductivity and
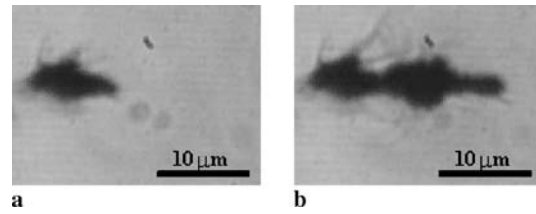

FIGURE 8 Graphitized structures fabricated in CVD diamond by 300-ps pulses: (**a**) one shot, (**b**) two shots

$C_p = 1800$ J/(kg K) is the heat capacity at $T = 1000$ K; $\varrho = 3.51 \times 10^3$ kg/m^3 is the material density [33]. The evaluated L_e^d and L_h are comparable with a size of the avalanche ionization zone ($L_e^b \approx 90$ nm); so, both the mechanisms of the energy dissipation must be taken into account under quantitative consideration. An actual rise of the modified region size due to post-pulse energy dissipation can be smaller or larger than the above estimations depending on the amount of the initial absorbed energy. The continuous growth regime dominates inside a narrow fluence range 0.35–1.2 J/cm^2, so we assume a weak influence of the energy dissipation process on the thickness of the modified layer.

Finally, we would like to consider the influence of the laser pulse duration on the process of bulk diamond microstructuring. It was mentioned already that the laser damage threshold for the 300-ps pulses fluctuates by a factor of two due to local material inhomogeneity compared with about 30% variation obtained for the 120-fs pulses. Another important feature of the long pulses is much higher growth rate in the continuous regime – up to 10 μm/shot. The typical graphitized structures fabricated inside the CVD diamond by one and two 300-ps pulses are shown in Fig. 8. Evident cracks in the surrounding diamond result, presumably, from huge dynamic mechanical stresses induced by fast expansion of a large material volume. The diameter of the modified region substantially changes over a single shot, correlating with the time variation of the local fluence during the triangle-like laser pulse. All these peculiarities evidence that using long picosecond pulses for the diamond bulk microstructuring is inappropriate.

4   Conclusions

The formation of microscopic regions with modified structure inside CVD diamond induced by multiple irradiation by 120-fs laser pulses at 800-nm wavelength has been studied experimentally. Highly efficient nonlinear absorption of femtosecond pulses in diamond ensures low sensitivity of the laser damage threshold to the structural defects, as follows from comparison of natural and CVD diamond. Raman spectroscopy confirms the graphitic nature of the laser-modified material. Local phase transition generates tensile stresses in the surrounding diamond, which, however, are not sufficient to cause material cracking.

Multiple laser irradiation results in appearance and spontaneous extension of the modified region from the focus towards the laser, so that separate graphitic globules and a continuous graphitic wire are consecutively formed in the general case. The mentioned varieties of structures feature different growth behavior, which has been explained by a change of the mechanism supplying seed electrons for the avalanche

impact ionization of diamond. The occurrence of separate graphitic globules is typical for high local fluence, when most seed electrons are generated directly in diamond due to non-linear absorption and accumulation of easily excited defects. On the contrary, continuous extension of the existing graphitized area appears predominant at low fluence. In this case, the avalanche ionization in a thin diamond layer near the graphitized area is initiated by photoexcited electrons penetrating into diamond from graphite. This regime in combination with a gradual shift of the focus position towards the laser makes possible fabrication of graphitic wires with typical length of $150\,\mu m$ and diameter of $1.5\,\mu m$.

Continuous graphitic structures can be produced inside CVD diamond by also applying longer, e.g. 300-ps, laser pulses. However, essential local fluctuations of the damage threshold, variation of the structure diameter over the length and pronounced cracking of the surrounding diamond make usage of long laser pulses much less attractive.

REFERENCES

1 J. Qiu, K. Miura, T. Suzuki, T. Mitsuyu, K. Hirao, Appl. Phys. Lett. **74**, 10 (1999)

2 K. Miura, J. Qiu, H. Inouye, T. Mitsuyu, K. Hirao, Appl. Phys. Lett. **71**, 3329 (1997)

3 K. Hirao, K. Miura, J. Non-Cryst. Solids **239**, 91 (1998)

4 O.M. Efimov, L.B. Glebov, K.A. Richardson, E. Van Stryland, T. Cardinal, S.H. Park, M. Couzi, J.L. Bruneel, Opt. Mater. **17**, 379 (2001)

5 Y. Shimotsuma, P.G. Kazansky, J. Qiu, K. Hirao, Phys. Rev. Lett. **91**, 247405 (2003)

6 K. Kawamura, T. Ogawa, N. Sarukura, M. Hirano, H. Hosono, Appl. Phys. B **71**, 119 (2000)

7 P. Srisungsitthisunti, O.K. Ersoy, X. Xu, Appl. Phys. Lett. **90**, 011104 (2007)

8 C.B. Schaffer, A.O. Jamison, E. Mazur, Appl. Phys. Lett. **84**, 1441 (2004)

9 S. Prawer, D.N. Jamieson, R. Kalish, Phys. Rev. Lett. **69**, 2991 (1992)

10 V.V. Kononenko, S.M. Pimenov, T.V. Kononenko, V.I. Konov, P. Fischer, V. Romano, H.P. Weber, A.V. Khomich, R.A. Khmelnitskiy, Diam. Relat. Mater. **12**, 277 (2003)

11 Y. Shimotsuma, M. Sakakura, S. Kanehira, J. Qiu, P.G. Kazansky, K. Miura, K. Fujita, K. Hirao, J. Laser Micro/Nanoeng. **1**, 181 (2006)

12 V.N. Strelalov, V.I. Konov, V.V. Kononenko, S.M. Pimenov, Appl. Phys. A **76**, 603 (2003)

13 V.V. Kononenko, T.V. Kononenko, S.M. Pimenov, M.N. Sinyavskii, V.I. Konov, F. Dausinger, Quantum Electron. **35**, 252 (2005)

14 V.G. Ralchenko, A.A. Smolin, V.I. Konov, K.F. Sergeichev, I.A. Sychov, I.I. Vlasov, V.V. Migulin, S.V. Voronina, A.V. Khomich, Diam. Relat. Mater. **6**, 417 (1997)

15 M. Lenzner, J. Krüger, S. Sartania, Z. Cheng, C. Spielmann, G. Mourou, W. Kautek, F. Krausz, Phys. Rev. Lett. **80**, 4076 (1998)

16 C.B. Schaffer, A. Brodeur, E. Mazur, Meas. Sci. Technol. **12**, 1784 (2001)

17 A.T. Collins, in *Handbook of Industrial Diamonds and Diamond Films* (Marcel Dekker, New York, 1998), p. 1

18 S. Preuss, M. Stuke, Appl. Phys. Lett. **67**, 338 (1995)

19 C.A. Klein, R. DeSalvo, Appl. Phys. Lett. **63**, 1895 (1993)

20 N.L. Boling, M.D. Crisp, G. Dube, Appl. Opt. **12**, 650 (1973)

21 A. Rosenfeld, M. Lorenz, R. Stoian, D. Ashkenasi, Appl. Phys. A **69**, S373 (1999)

22 T.V. Kononenko, V.G. Ralchenko, I.I. Vlasov, S.V. Garnov, V.I. Konov, Diam. Relat. Mater. **7**, 1623 (1998)

23 R.W. Boyd, *Nonlinear Optics* (Academic Press, Boston, 1992)

24 L. Sudrie, M. Franco, B. Prade, A. Mysyrowicz, Opt. Commun. **191**, 333 (2001)

25 A.M. Zaitsev, in *Handbook of Industrial Diamonds and Diamond Films* (Marcel Dekker, New York, 1998), p. 227

26 J.W. Ager, M.D. Drory, Phys. Rev. B **48**, 2601 (1993)

27 V.G. Ralchenko, E.D. Obraztsova, K.G. Korotushenko, A.A. Smolin, S.M. Pimenov, V.G. Pereverzev, Mater. Res. Soc. Symp. Proc. **383**, 153 (1995)

28 D.S. Olson, G.J. Reynolds, G.F. Virshup, F.I. Friedlander, B.G. James, L.D. Partaina, J. Appl. Phys. **78**, 5177 (1995)

29 S.D. Brorson, J.G. Fujimoto, E.P. Ippen, Phys. Rev. Lett. **59**, 1962 (1987)

30 T. Malinauskas, R. Aleksiejunas, B. Monemar, V. Ralchenko, A. Gontar, E. Ivakin, K. Jarasiunas, thesis for *International Conference on SiC and Related Materials (ICSCRM)*, Otsu, Japan, 2007

31 E.G. Gamaly, A.V. Rode, B. Luther-Davies, V.T. Tikhonchuk, Phys. Plasmas **9**, 949 (2002)

32 H.E. Elsayed-Ali, T.B. Norris, M.A. Pessot, G.A. Mourou, Phys. Rev. Lett. **58**, 1212 (1987)

33 V.I. Nepsha, in *Handbook of Industrial Diamonds and Diamond Films* (Marcel Dekker, New York, 1998), p. 147